

## DURABILITY OF PULTRUDED GLASS-FIBER-REINFORCED POLYESTER PROFILES FOR STRUCTURAL APPLICATIONS

**J. R. Correia,\* S. Cabral-Fonseca,\*\*  
F. A. Branco,\*\* J. G. Ferreira,\*  
M. I. Eusébio,\*\* and M. P. Rodrigues\*\***

**Keywords:** *glass-fiber-reinforced polyester, pultrusion, environmental degradation, chemical properties, mechanical properties, physical properties*

*Results of an experimental research into the physical, chemical, mechanical, and aesthetical changes suffered by pultruded glass-fiber-reinforced polyester profiles during their testing for accelerated aging under the action of moisture, temperature, and ultraviolet (UV) radiation are presented. The profiles were submitted to the influence of four different exposure environments: (i) in an immersion chamber, (ii) in a condensation chamber, (iii) in a QUV accelerated weathering apparatus, and (iv) in a xenon-arc accelerated weathering apparatus. The results obtained were analyzed regarding the changes in their weight, sorption ability, tensile and flexural strength characteristics, color, and gloss; the chemical changes were investigated by means of Fourier-transform infrared spectroscopy. Considerable chromatic changes were observed, especially owing to the UV radiation. Although some reduction in the mechanical properties was observed, particularly in the immersion and condensation chambers, the durability tests proved a generally good behavior of this material under the aggressive conditions considered.*

### Introduction

Pultruded glass-fiber-reinforced polymer (GFRP) profiles have a great potential for structural applications owing to some of their advantages over traditional materials, namely the higher strength to weight ratio, the lower weight, the electromagnetic transparency, the ease of installation, the lower maintenance requirements, and the improved durability in aggressive environments.

Up to now, GFRP profiles have been used mainly in nonstructural or secondary structural elements, such as ladders, handrails, and pavement grids. Their use in load-carrying structural elements, except for a few demonstration projects of pedestrian bridges (Fig. 1 [1]), highway bridges, and buildings, is still limited to the fields of application with specific requirements of lightness or corrosion resistance, such as the oil, chemical, and water treatment industries.

Paradoxically, one of the factors delaying the widespread acceptance of GFRP profiles as load-carrying structural elements is the lack of comprehensive and validated data on their durability [2], because the service life of construction infrastructures is generally expected to exceed 50 years. Furthermore, this factor has been recently identified by several authors as the

---

\*Instituto Superior Técnico, Technical University of Lisbon, Lisboa, Portugal. \*\*Laboratório Nacional de Engenharia Civil, Lisboa, Portugal. Russian translation published in *Mekhanika Kompozitnykh Materialov*, Vol. 42, No. 4, pp. 463-474, July-August, 2006. Original article submitted October 25, 2005; revision submitted January 18, 2006.



Fig. 1. GFRP footbridge in Lerida, Spain [1].

most critical gap between the needed and available information regarding the future research [2, 3], particularly for composites produced by large-scale processing methods, such as pultrusion.

In order to clarify the durability of GFRP structural elements, this paper presents the results of an experimental research into the physical, chemical, mechanical, and aesthetical changes suffered by pultruded GFRP profiles during their testing for accelerated aging under the action of moisture, temperature, and ultraviolet (UV) radiation. The test specimens were cut from commercial pultruded GFRP profiles currently used for infrastructure applications. They were submitted to the influence of four different exposure environments: (i) in an immersion chamber, (ii) in a condensation chamber, (iii) in a QUV accelerated weathering apparatus, and (iv) in a xenon-arc accelerated weathering apparatus. Thereafter their sorption behavior was analyzed, the tensile and flexural behavior was studied, the chromatic and gloss variations were measured, and the chemical changes were investigated by means of Fourier-transform infrared (FTIR) spectroscopy.

## 1. Materials

The material studied was obtained from two current commercial pultruded I-shaped GFRP profiles, A and B, both produced by Topglass. This material consists of alternating layers of unidirectional E-glass fiber rovings and strand mats embedded in isophthalic polyester resin. The content of mineral fraction, determined from burn-off experiments according to the ISO 1172 standard [4], was 62 vol.%.

Specimens of dimensions 10 15 300 mm were cut from profile A in the longitudinal direction and used in different tests (three to five specimens for each period and condition of exposure). From profile B, specimens were also cut in the longitudinal direction, but with various dimensions, according to the nature of the test to be performed (five specimens for each period and condition of exposure).

## 2. Methods

**2.1. Exposure environments.** In order to study the possible degradation of the material in environments typical of civil engineering applications, the specimens were subjected to the following tests.

(i) In an immersion chamber, where specimens from profile A were held in water at a constant temperature of 20 °C for up to 6480 h.

(ii) In a condensation chamber, where specimens from profile A were exposed to constant condensation of deionized water at a constant temperature of 60 °C for up to 6480 h.

(iii) In a QUV accelerated weathering apparatus, where specimens from both the profiles were exposed to repeating cycles of light and moisture, produced by condensation of water under controlled conditions. The cycles, according to ISO 4892, part 3 [5] recommendations, consisted of a 4-h permanent exposure to solar radiation simulated with fluorescent lamps at

60 °C, and a 4-h exposure to moisture caused by constant condensation of deionized water at 50 °C for up to 6346 h for profile A and 2000 h for profile B. The fluorescent lamps used in the QUV chamber were of type UVA-340, providing an irradiance of  $0.77 \text{ W}/(\text{m}^2 \cdot \text{nm})$  at 340 nm, which reproduced the most relevant part of solar spectrum between 290 and 350 nm. The lamps were periodically repositioned (with a 400-h interval between rotations) in order to provide a uniform radiation for all the test specimens.

(iv) In a xenon-arc light accelerated weathering apparatus, where the specimens from profile B were exposed, for up to 2000 h, according to a predetermined program consisting of a continuous irradiation with intermittent cycles of water spray under controlled conditions. The light source and the respective borosilicate glass filters provided a spectral irradiation of  $0.50 \text{ W}/(\text{m}^2 \cdot \text{nm})$  at 340 nm, which reproduced some harmful effects of sunlight on this type of material. The relative humidity during the dry part of the cycle was 65%, and the black-body temperature inside the chamber was 65 °C. The duration of water sprays was 18 min with 102-min dry intervals between spraying, according to ISO 4892, part 2 [6].

**2.2. Experimental procedures.** At preassigned intervals of time, the test specimens placed in the different exposure environments were removed for physical, chemical, mechanical, and aesthetical characterization, which included the study of their (i) water absorption, (ii) weight changes, (iii) tensile properties, (iv) flexural properties, (v) color variation, (vi) gloss variation, and (vii) chemical changes by means of infrared spectroscopy.

For water absorption investigations, the specimens from profile B were removed from deionized water at preassigned intervals up to 5544 h of exposure.

For all the other experimental procedures, after removing from the different exposure environments, the specimens were placed in a chamber at 20 °C and 50% relative humidity, with consecutive weighting (with a precision of 0.01 g) until a constant weight was reached (when the relative differences between successive measurements at 24-h intervals were less than 0.1%).

The specimens from profile A were taken out of test chambers after 2160, 4320, and 6480 h of exposure of the specimens placed in the immersion and condensation chambers and after 1642, 3304, 4839, and 6346 h of exposure of those placed in the QUV chamber. The specimens from profile B placed in the QUV chamber were removed after 1000 h of exposure, and those placed in the xenon-arc chamber were removed after 1000 and 2000 h of exposure.

**2.2.1 Water absorption (profile B) and weight changes (profile A).** The water absorption of profile B was measured following the procedures specified by ISO 62 [7]. Specimens of dimensions  $75 \times 25 \times 8$  mm were immersed in deionized water and left to stand at a constant temperature of  $23 \pm 1^\circ\text{C}$ . The amount of water absorbed by the GFRP specimens was determined by monitoring its change in weight (weight gain) over the time up to 5544 h of exposure. Prior to the water absorption experiments, the test specimens were dried in an oven at 50 °C until a constant weight and then cooled in a desiccator.

In order to determine the weight changes (the effect of residual moisture) under the conditions of each environment, for different times of exposure, the specimens from profile A were weighed at preassigned time intervals, after a constant mass was reached at the ambient temperature ( $23 \pm 1^\circ\text{C}$ ).

**2.2.2. Tensile tests (profile B).** Rectangular  $8 \times 20 \times 250$ -mm specimens from profile B were tested in tension according to International Standard ISO 527, parts 1 and 5 [8], without end-tabs, after 2000 h of exposure in the QUV chamber and after 1000 and 2000 h of exposure in the xenon-arc chamber.

Specimens corresponding to each exposure environment and duration were loaded monotonically up to failure, at a displacement rate of 2 mm/min. A strain gage was attached to the test specimens, and the data obtained were analyzed to determine the tensile properties (the strength, Young's modulus, and the strain at break) of both unaged and aged specimens.

**2.2.3. Flexural tests (profile A).** Flexural tests (3-point) were conducted according to ISO 14125 [9] on specimens obtained from profile A in order to determine the effect of degradation caused by the different exposure environments on their flexural properties. Specimens with a span-to-depth ratio of 20 were loaded at an approximate speed of 4 mm/min. Load and displacement data were continuously measured and recorded during the experiments. Specimens were tested to failure, and the data obtained were analyzed to determine the flexural properties (the strength, Young's modulus, and the strain at failure) of both unaged and aged specimens.

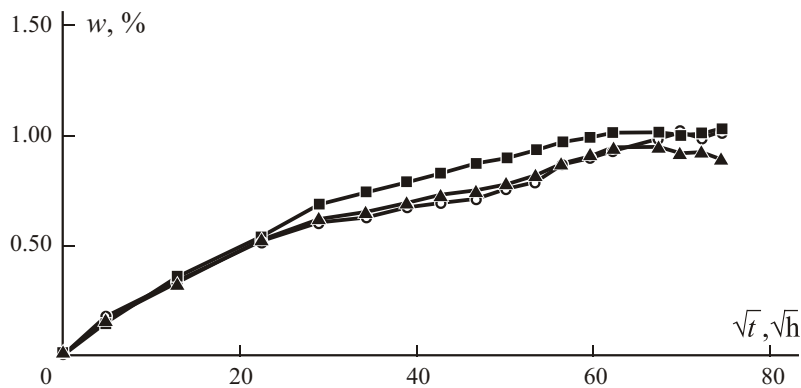


Fig. 2. Water absorption ratio  $w$  (profile B) for specimen 1 (○), specimen 2 (■), and specimen 3 (▲).

2.2.4 *Color differences (profiles A and B)*. The color differences caused by the different environments were measured with a Macbeth Color Eye 3000 spectrophotometer in the reflection mode with the specular component excluded and the spectral ultraviolet energy included.

For profile A, the color measurements were performed on the exposed surface of the specimens used for flexural tests, while for profile B, the colorimetric measurements were performed using always the same 8 × 50 × 100-mm plate. This plate, which was aged in the same way as the other test specimens under the different UV radiation exposures, was used only for the nondestructive tests (color and gloss measurements). The color differences were determined in relation to the unaged material.

The results obtained were expressed in terms of the CIE  $L^*a^*b^*$  system according to the International Standard ISO 7724 test method for the colorimetry of paints and varnishes [10]. In this system, the values of  $L^*$  give the measurement of lightness, and the values of  $a^*$  and  $b^*$  give the measurements of color in the red–green axes and yellow–blue axes, respectively. The changes in color were described in terms of the variations  $\Delta L^*$ ,  $\Delta a^*$ ,  $\Delta b^*$ , and  $\Delta E^*$ , where the last parameter expresses the measurement of the overall color change.

2.2.5. *Gloss variation (profile B)*. Gloss measurements were carried out using a Rhopoint-Statistical Novo-gloss model glossmeter set at an angle of incidence/reflection of 60°. The results presented are the mean values of six readings per test specimen.

2.2.6. *Infrared spectroscopy (profiles A and B)*. In order to study the chemical changes of the surface of test specimens subjected to different environmental exposures, infrared spectra were measured by using a Fourier transform infrared analysis performed on a Nicolet Magna 550 spectrometer. The samples were scraped from the exposed surfaces of aged specimens, mixed with dry spectroscopic grade potassium bromide and pressed into pellets. Thirty two scans were collected and averaged at a spectral resolution of 4  $\text{cm}^{-1}$ . The spectra were rationed against the background spectrum, which was previously measured to remove the effects of the background in the pellets tested.

The occurrence of chemical reactions during different environments was investigated by studying the relative intensities of the principal infrared absorption peaks susceptible to changes during aging. In order to make comparisons between the composite specimens subjected to different periods and types of aging, the absorbance of each peak was referred to the absorption of the band at 1452  $\text{cm}^{-1}$ . This band can be attributed to the bending of the C–H segment of  $\text{CH}_2$ . This peak seemed to occur in all specimens, which justified its choice as a reference band.

### 3. Results and Discussion

The evolution of GFRP properties with exposure time, for specific environments, is commonly used as a measure of the extent of deterioration caused by aging. Therefore, variations or the retention ratios (ratios between the values of properties

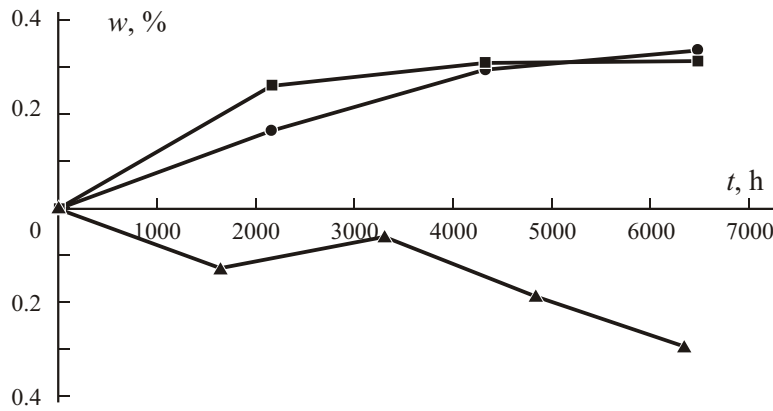


Fig. 3. Weight change ratio  $w$  vs. the exposure period  $t$  in different environments: in 20 C water (●), in 60°C water (■), and in the QUV apparatus (▲).

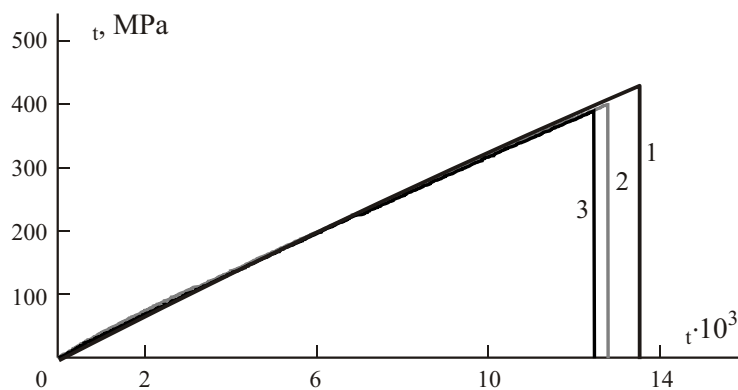


Fig. 4. Tensile stress–strain curves  $\sigma_t$  ( $\epsilon_t$ ) of representative specimens for different exposure environments: unaged (1), in the QUV apparatus (2000 h) (2), and in the xenon-arc apparatus (2000 h) (3).

for aged and unaged specimens) of some material properties (physical, chemical, mechanical, and aesthetic) will be presented as durability indicators of the material tested in the exposure environments used in this study.

**3.1 Water absorption (profile B) and weight changes (profile A).** Some researchers have reported a great influence of the equilibrium and rate of water absorption on the thermophysical, mechanical, and chemical properties of polymer composites [11-13]. The amount of absorbed water greatly depends on the chemical composition, the morphology, and the degree of curing of the polymeric matrix of the composites. The water content may induce physical and chemical aging, or a combination of both, which can be reversible, partially reversible, or irreversible, depending on the nature of the material and the period and conditions of exposure. Usually, weight changes in moist environments result from the balance between the weight gain due to water absorption and the weight loss due to the extraction of low-molecular components.

As seen in Fig. 2, the curve of weight gain  $w$  versus square root of immersion time  $t$  shows an initial linear segment followed by a flatter section, which can be roughly described as Fickian in nature. However, despite the gradually decrease in the rate of water absorption, the equilibrium plateau was not reached. The unclear saturation level reflects the complexity of water uptake in heterogeneous materials such as the GFRP profiles. In fact, the water uptake by composites can involve different mechanisms: (i) diffusion of water molecules directly into the matrix and, to a much lesser amount, into the fiber material; (ii) capillary flow of water along the fiber-matrix interface; and (iii) transport of water through microcracks or other forms of small damages, such as pores or minute channels already present in the material or expanded by water [14].

Figure 3 shows changes in the specimens weight  $w$  as a function of deterioration period  $t$  for different exposure environments. In the immersion and condensation chambers, the overall weight gain was 0.34 and 0.31%, respectively. It appears

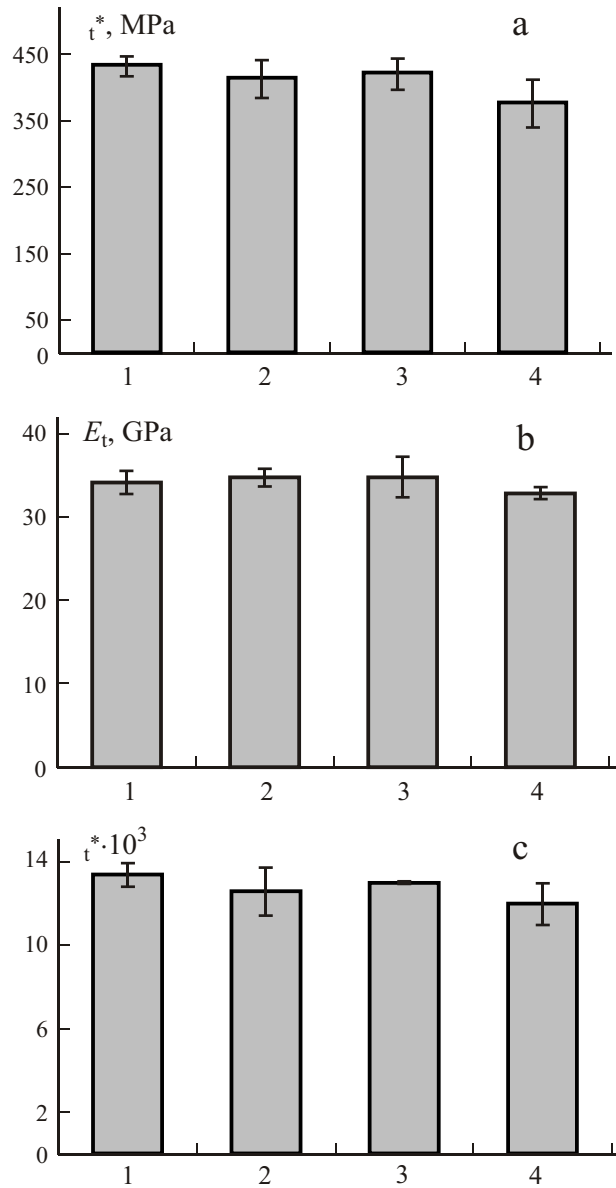


Fig. 5. Tensile strength  $\sigma_t$  (a), Young's modulus  $E_t$  (b), and strain at break  $\epsilon_t$  (c) for different exposure environments and durations (profile B): unaged (1), in the QUV apparatus for 2000 h (2), and in the xenon-arc apparatus for 1000 (3) and 2000 h (4).

that a quasi-equilibrium state was reached, especially in the condensation chamber. The higher initial rate of water uptake in the condensation chamber was probably caused by the increased temperature of the environment. This result is consistent with other results at elevated temperatures for different types of polymer composites [15, 16]. In the QUV chamber, the weight variation was opposite, namely an overall weight loss of 0.29% was observed, showing that the weight loss due to the extraction of molecular components was more important than the weight gain due to water absorption during condensation cycles, which took place for only half the total period of exposure.

**3.2 Tensile properties (profile B).** Figure 4 shows the experimental tensile stress-strain curves – of representative specimens for different exposure environments. Both for unaged (control specimens) and aged specimens, the curves are almost perfectly linear up to failure, which can be considered valid according to [8]. The results of all tensile tests are plotted in Fig. 5, where  $\sigma_t$  is the tensile strength,  $E_t$  is the tensile Young's modulus, and  $\epsilon_t$  is the tensile strain at break.

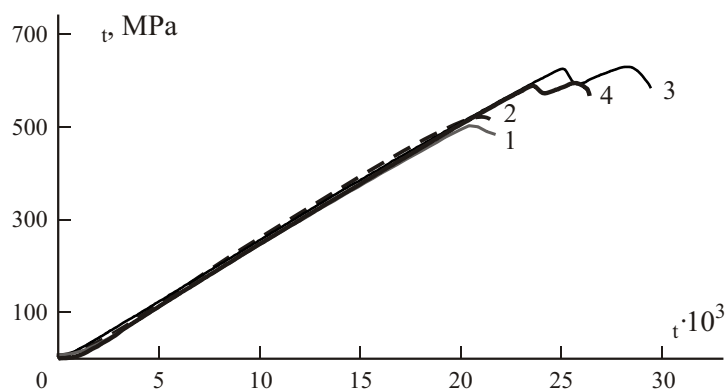


Fig 6. Flexural stress–strain curves  $\sigma_f(\epsilon_f)$  of representative specimens for different exposure environments: unaged (1), immersion (6480 h) (2), condensation (6380 h) (3), and QUV (6346 h) (4).

An overall decrease in the average tensile strength with increasing exposure time was observed for all the environments. However, after 2000-h and 1000-h exposures in the QUV and xenon apparatus, respectively, the strength decrease was small (4 and 3%, respectively). A slightly more significant strength decrease (13%) was observed after the 2000-h exposure in the xenon apparatus. Nonetheless, considering the magnitude of error bars (representing one standard deviation), the differences are not statistically significant.

It is likely that the larger extent of degradation caused by the xenon apparatus compared with that induced by the QUV equipment is not due to the UV radiation but due to the kinetic effect of water sprays on the specimens surface, which may have accelerated the material degradation. In fact, of both the apparatus, QUV produces a higher irradiance at 340 nm (which constitutes the most harmful part of solar spectrum for polymer debonding), while the xenon apparatus provides a broader spectral irradiance.

The strain at failure shows a similar pattern of variation, with almost no reduction after the 2000-h and 1000-h exposures in the QUV and xenon apparatus, respectively, and a slight reduction (8%) after the 2000-h exposure in the xenon apparatus.

The tensile modulus remained largely unaffected for both the types of exposure, with a marginal increase (2%) and a very slight decrease (4%) after the 2000-h exposure in the QUV and xenon apparatus, respectively.

**3.3. Flexural properties (profile A).** Figure 6 shows the stress–strain curves – obtained in flexural tests on representative specimens for different exposure environments. All the specimens exhibited quite a linear behavior up to failure with very similar stress–strain curves. The results of the flexural tests performed after the exposure of specimens to different aging conditions are plotted in Fig. 7, where  $\sigma_f$  is the flexural strength,  $E_f$  is the flexural Young’s modulus, and  $\epsilon_f$  is the flexural strain at failure.

A noticeable decrease in the flexural strength was observed under the immersion and condensation exposure conditions, where flexural strength retentions of 84 and 81%, respectively, were observed after a 6480-h exposure. This decrease occurred especially after the first period (2160 h) of exposure (87 and 84% retention, respectively), while the reduction in the final period (2160 to 6480 h) was only 3% in those exposure environments. For specimens aged in the QUV chamber, the flexural strength seems to have been unaffected. After a 6% drop in the first 1642 h, the flexural strength increased continuously up to a 98% retention after 6346 h of exposure.

The reduction in the strain at failure presents a similar pattern to that of the flexural strength: 87% and 82% retention were observed after 6480 h of exposure under the immersion and condensation exposure conditions, respectively. In the environments with the UV radiation exposure (QUV and xenon apparatus), the strain at failure was almost unaffected for both the profiles.

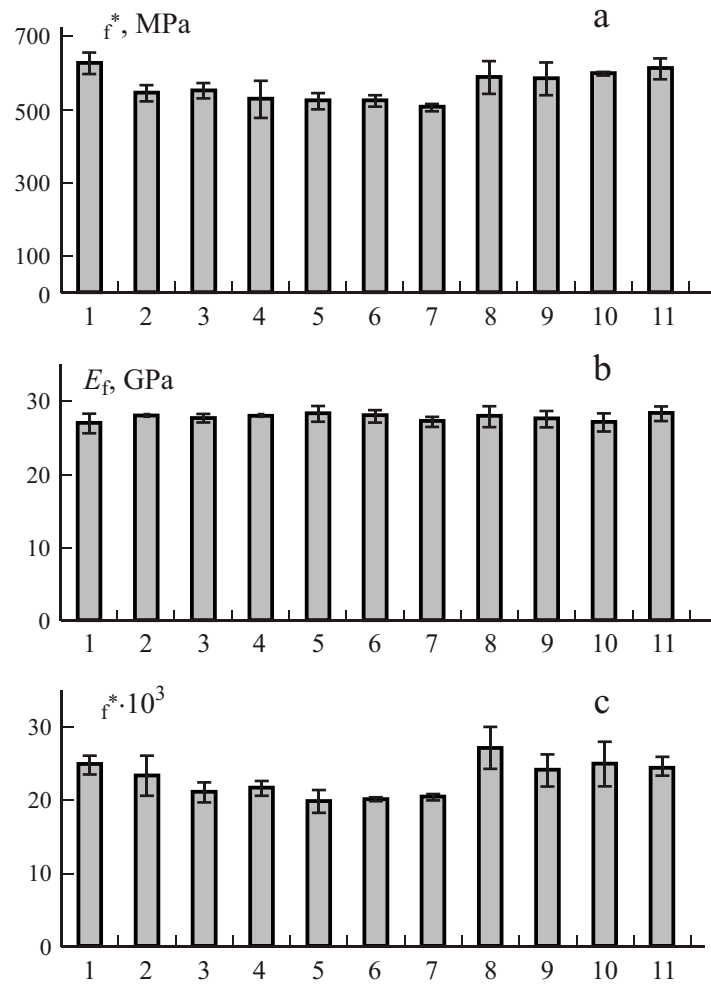


Fig. 7. Flexural strength  $f_f$  (a), Young's modulus  $E_f$  (b), and strain at failure  $f_f$  (c) for different exposure environments and durations (profile A): unaged (1), 20°C water for 2160 h (2), 20°C water for 4320 h (3), 20°C water for 6480 h (4), 60°C water for 2160 h (5), 60°C water for 4320 h (6), 60°C water for 6480 h (7), QUV for 1642 h (8), QUV for 3304 h (9), QUV for 4839 (10), and QUV for 6346 h (11).

The flexural modulus also remained practically the same after the exposure to the different environments. Very slight stiffness increases, 4 and 1%, were detected after the 6480-h exposure in the immersion and condensation chambers, respectively, and a 5% increase was observed after the 6346-h exposure in the QUV apparatus. These results are in agreement with the experiments performed by Liao et al. on a glass-fiber-reinforced vinyl ester [15] and by Kajorncheappunngam et al. on a glass-fiber-reinforced epoxy [17]. This behavior is due to the fact that the flexural modulus of glass-fiber-reinforced polymers is affected only by temperatures close to the glass-transition temperature of the polymers. Moreover, according to Apicella et al. [18], there exist a competitive effect between the plasticization of matrix as a result of water absorption and the stiffness increase due the loss of low-molecular-weight substances.

The reduction in the strain at failure in the immersion and condensation chambers is an indicator of polymer degradation due to water absorption. The water absorption also had a noticeable influence on the reduction in the flexural strength, and this effect was accelerated by temperature. Similar results were obtained by Nishizaki and Meiarashi [16] and Van de Velde et al. [19] for a pultruded glass-fiber-reinforced polyester. Regarding the UV radiation, our results seem to confirm that the effects of this exposure agent are usually confined to the top few micrometers of the surface and therefore have only a limited influence



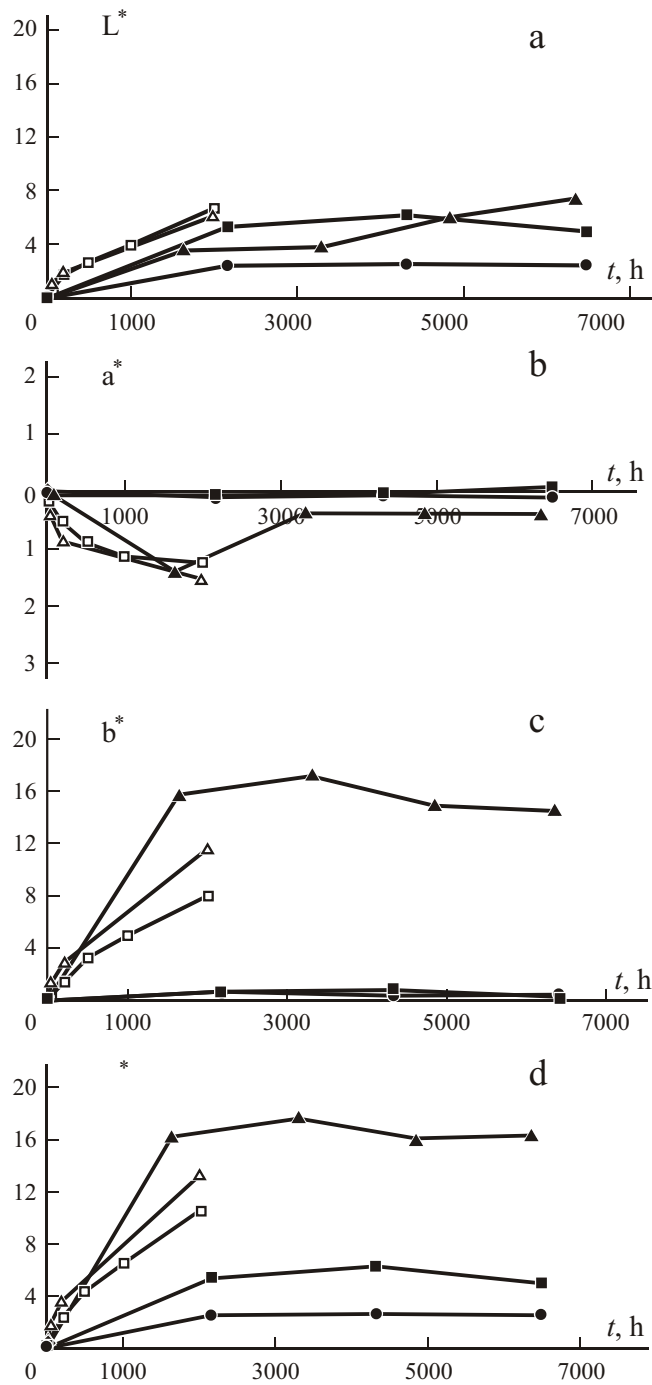


Fig. 8. Variations in the color parameters  $L^*$  (a),  $a^*$  (b),  $b^*$  (c),  $E^*$  (d) in relation to the exposure time  $t$  in 20°C water (A) (●), 60°C water (A) (■), QUV(A) (▲), QUV (B) (△), and xenon-arc apparatus (B) (□).

on the mechanical properties of the material [20, 21]. Although the UV radiation may cause surface deterioration, thus increasing the degradation potential of moisture and other aggressive agents, it is unlikely that the thick GFRP profiles currently used in construction could be directly affected by the UV radiation.

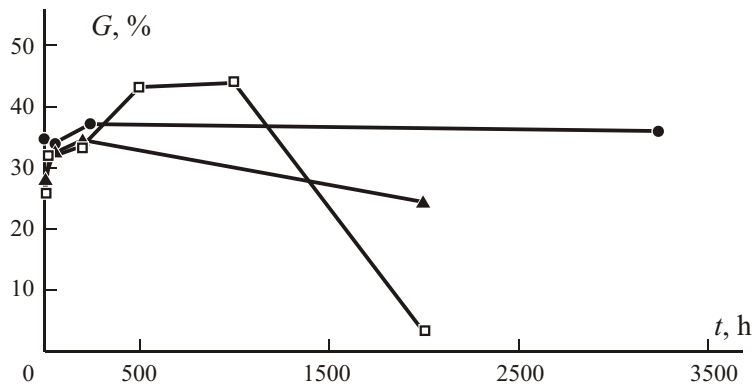


Fig. 9. Gloss variation  $G$  in the time  $t$  for profile B in the QUV (▲) and xenon-arc apparatus (□) and in the reference specimen (●).

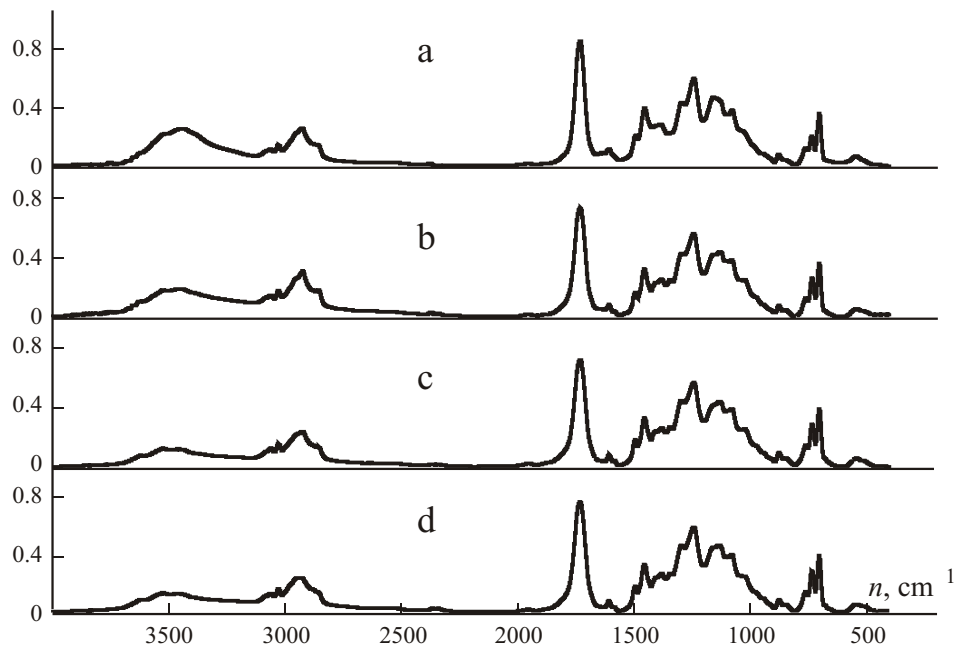


Fig. 10. Infrared spectra of profile A for the reference specimen (a) and for the specimens placed in the immersion chamber for 2160 (b), 4320 (c), and 6480 h (d);  $n$  is the relative absorbance.

**3.4. Color differences (profiles A and B).** The chromatic variations in the specimens of both profiles occurring in the immersion, condensation, QUV, and xenon chambers are shown in Fig. 8 in relation to the exposure environment and duration, where  $L^*$ ,  $a^*$ ,  $b^*$ , and  $E^*$  are the variations in the corresponding coordinates.

In the immersion chamber, the chromatic variations were insignificant and consisted mainly of a weak surface brightening and a very slight increase in yellowness. In the condensation chamber, the chromatic variations followed the same pattern of surface brightening and yellowness increase, but to a greater extent. The most significant chromatic variations were registered for the specimens aged in the UV radiation chambers (QUV and xenon-arc apparatus). A slight increase in the green color, a brightness increase and, above all, a marked increase in yellowness, which was clearly visible by the naked eye, were observed.

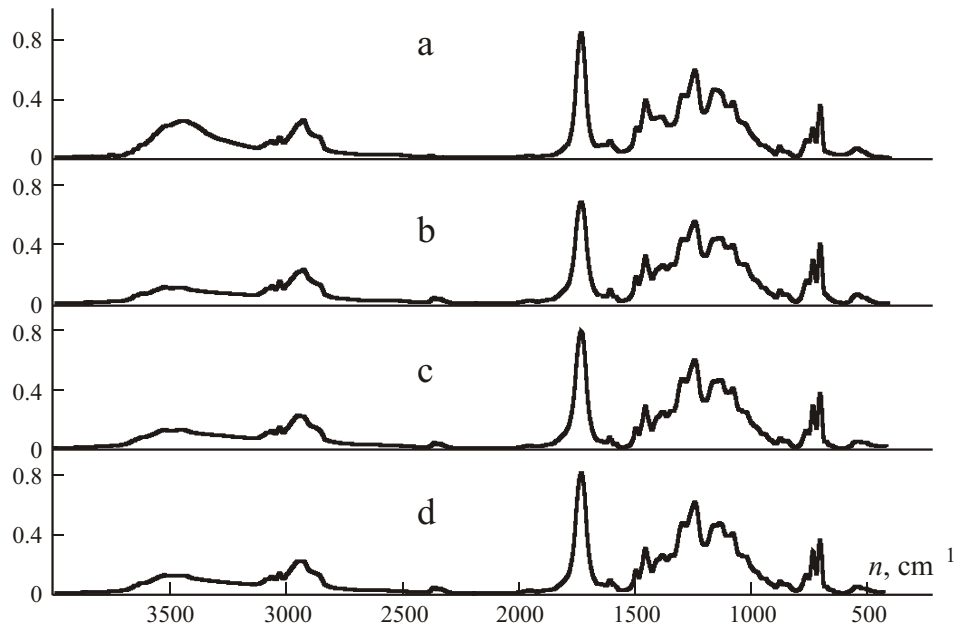


Fig. 11. The same for the specimens placed in the condensation chamber.

The chromatic variations seen in the specimens subjected to aging in the condensation chamber, and especially in the QUV and xenon chambers, present an obvious esthetical concern regarding outdoor applications. However, under all the aging conditions, the chromatic variations stabilized after a short period of exposure. This aspect may be considered when structural elements of a construction have to be replaced, as the replacing elements will rapidly acquire the same aspect.

**3.5 Gloss variation (profile B).** The gloss variation  $G$  of the specimens obtained from profile B and placed in the QUV and xenon equipments is shown in Fig. 9 as a function of the type and duration  $t$  of exposure.

After an initial increase in gloss for both the UV exposure environments, probably owing to the polishing of specimen surface, the gloss started to decrease. The highest decrease in gloss was found after 2000 h of exposure in the xenon apparatus, with a gloss loss of about 87% compared with that of unaged test specimens.

All test specimens revealed a change in appearance, either in color (as described above) or in gloss. These changes, which were insignificant for the specimens aged in the immersion and condensation chambers, could be easily visible by the naked eye for the specimens submitted to UV radiation. Similar results were obtained by Bogner and Borja for pultruded profiles made from isopolyester and vinylester resins reinforced with glass fibers [21].

The results reported here show that the most important effect of UV radiation in pultruded GFRP profiles is the gloss loss and change in color (mainly the yellowing of the materials surface). These UV effects, which are restricted to a limited near-surface thickness of the material and are mainly cosmetic, do not seem to affect the mechanical performance of GFRP profiles significantly.

**3.6 Infrared spectroscopy (profiles A and B).** Figures 10 and 11 show the spectra of the specimens obtained from profile A and submitted to the immersion and condensation exposures, respectively, where  $n$  is the wavenumber. Figures 12 and 13 show the spectra of the specimens obtained from profiles A and B, respectively, and submitted to the environments with UV radiation.

The spectra obtained from the specimens placed in the immersion and condensation environments revealed changes in some absorptions bands during aging, namely modifications in the intensities of absorption peaks, especially for longer durations of aging. In both the environments, the intensity of the carbonyl peak ( $1730\text{ cm}^{-1}$ ) decreased, more markedly in the case of immersion (13%) than condensation (5%), probably due to the slight leaching of the low-molecular-weight carboxylic constituents soluble in water. During aging in these environments, changes in the height ratio of the peaks corresponding to styrene ( $701\text{ cm}^{-1}$ ) and phthalate ( $732\text{ cm}^{-1}$ ) were also observed. This fact was confirmed by the decreasing intensity of the styrene

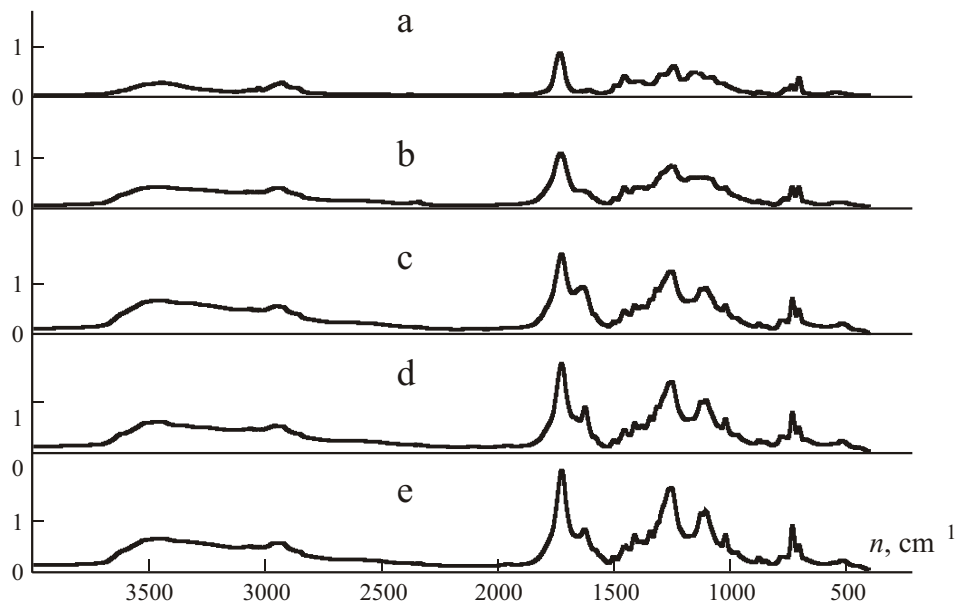


Fig. 12. Infrared spectra of profile A for the reference specimen (a) and the specimens placed in the QUV apparatus for 1642 (b), 3304 (c), 4839 (d), and 6480 h (e).

characteristic band at  $3027\text{ cm}^{-1}$  and can be explained by the loss of styrene, most likely the residual monomer, with time. This phenomenon was already observed in previous studies [22]. Some authors have mentioned the occurrence of chemical attack on the ester linkage of unsaturated polyester resin of the composite matrix after long periods of water exposition at elevated temperatures, but in our experiments, this type of changes was not detected.

In the IR spectra formed on the surface of the test specimens exposed to the environments with UV radiation, there were indications of chemical changes, revealed by modifications in the intensity and shape of some absorption peaks, as well as by the rise of new ones, especially for longer durations of aging. During the QUV exposure, the intensity of the carbonyl band ( $1730\text{ cm}^{-1}$ ) increased, and after 6480 h it was 42% higher than that of the reference specimen. In the xenon camera, in spite of the shorter duration of aging, the intensity of the carbonyl band increased by 49%. In both the cases, the increased intensity of the carbonyl peak was followed by its widening. As in the environments analyzed previously, in the QUV and xenon aging, there was also observed a decrease in the styrene content, which showed up as a decrease in the intensity of the characteristic bands. New bands also appeared, namely at  $1630\text{ cm}^{-1}$ , which could be caused by the formation of conjugated double C=C bonds. These bonds can explain the yellowness observed for the specimens subjected to UV radiation [23]. The chemical alterations observed result from the photodegradation of the unsaturated polyester. This phenomena was studied in [24] and proved to involve chain scission, cross-linking, and yellowing [24].

The results obtained show that the effects of UV exposure are usually confined to the top few micrometers of specimen surface, leading only to a minor change in its mechanical properties, as mentioned previously. This is particularly true for thick structural members used in construction, in which the degradation affects only their thin outer layer.

## Conclusions

Based on the findings of this study, the following conclusions can be drawn, which are related to the use of pultruded glass-fiber-reinforced polyester profiles in construction:

1. Immersion and condensation environments effect the flexural properties of GFRP profiles. Moisture can decrease their strength and strain at failure by up to 20%, and this effect is accelerated by increased temperatures. The degradation is caused mainly by physical phenomena, such as plasticization of the polymeric matrix, since no appreciable chemical degrada-

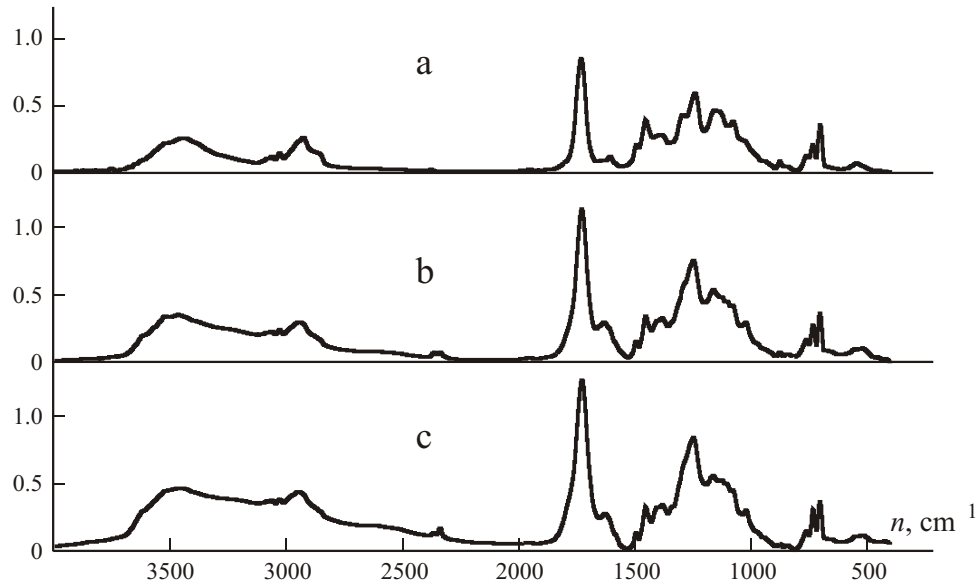


Fig. 13. Infrared spectra of profile B for the reference specimen (a) and the specimens placed in the QUV (b) and xenon-arc apparatus (c) for 2000 h.

tion was detected by the FTIR analysis. Nevertheless, this degradation may influence the use of GFRP profiles with polyester resins in wet environments (structures placed underwater or subjected to high levels of moisture) and especially in tropical zones (with higher temperatures), where the use of different resin systems must be considered for improved performance.

2. Although the FTIR analysis showed a noticeable chemical degradation in the surface of the material in the QUV and xenon arc experiments, the synergetic effects of simultaneous exposure to the UV radiation, moisture, and temperature on the flexural and tensile properties of GFRP profiles were insignificant during the experiment. These results seem to confirm that the UV radiation has a limited influence on the mechanical properties of the material, affecting mainly the surface of the material and its aesthetical properties.

3. The considerable chromatic and gloss changes observed, especially due to the UV radiation, cause an aesthetical concern for outdoor applications, where the use of protective coatings can hardly be avoided.

4. Globally, this research has shown that, although some caution must be exercised in dealing with construction elements subjected to the UV radiation to prevent the possible aesthetical changes in them, pultruded GFRP profiles offer a very good mechanical performance and lightness, as well as good durability characteristics, compared with those of traditional structural materials.

## REFERENCES

1. J. Sobrino and M. D. Pulido, "Towards advanced composite materials footbridges," *Struct. Eng. Int., IABSE*, **12**, No. 2, 84-87 (2002).
2. V. M. Kharbari, J. W. Chin, D. Hunston, B. Benmokrane, T. Juska, R. Morgan, J. J. Lesko, U. Sorathia, and D. Reynaud, "Durability gap analysis for fiber-reinforced polymer composites in civil infrastructure," *J. Compos. Construct.*, **7**, No. 3, 238- 247 (2003).
3. K. A. Harries, M. A. Porter, J. P. Busel, "FRP materials and concrete research needs," *Concrete Int., ACI*, 69-74 (October, 2003).
4. ISO 1172: Textile-Glass-Reinforced Plastics — Prepregs, Moulding Compounds and Laminates — Determination of the Textile-Glass and Mineral Filler Content — Calcination Methods (1996).

5. ISO 4892: Plastics: Methods of Exposure to Laboratory Light Sources. Pt. 1: General Guidance. Pt. 3: Fluorescent UV Lamps (1994).
6. ISO 4892: Plastics: Methods of Exposure to Laboratory Light Sources. Pt. 1: General Guidance. Pt. 2: Xenon-arc Sources (1994).
7. ISO 62: Plastics: Determination of Water Absorption (1999).
8. ISO 527: Plastics: Determination of Tensile Properties. Pt. 1: General Principles. Pt. 5: Test Conditions for Unidirectional Fiber-Reinforced Plastic Composites (1997).
9. ISO 14125: Fiber-Reinforced Plastic Composites — Determination of Flexural Properties (1998).
10. ISO/DIS 7724-1: Paints and Varnishes — Colorimetry. Pt. 1: Principles. Pt. 2: Colour Measurement. Pt. 3: Calculation of Colour Differences by CIELAB (1997).
11. K. Liao, C. R. Schultheisz, D. L. Hunston, and L. C. Brinson, "Long-term durability of fiber-reinforced polymer matrix composite materials for infrastructure applications: a review," *J. Adv. Mater.*, **30**, No. 4, 3-40 (1998).
12. C. L. Schuttle, "Environmental durability of glass-fiber composites," *Mater. Sci. Eng.*, **13**, No. 7, 265-323 (1994).
13. J. W. Chin, T. Nguyen, and K. Aouadi, "Effects of environmental exposure on fiber-reinforced plastic (FRP) materials used in construction," *J. Compos. Technol. Res.*, **19**, No. 4, 205-213 (1997).
14. E. Boinard, R. A. Pethrick, J. Dalzel-Job, and C. J. Macfarlane, "Influence of resin chemistry on water uptake and environmental ageing in glass fiber reinforced composites — polyester and vinyl ester laminates," *J. Mater. Sci.*, **35**, 1931-1937 (2000).
15. K. Liao, C. R. Schultheisz, and D. L. Hunston, "Effects of environmental aging on the properties of pultruded GFRP," *Composites, Pt. B, Eng.*, **30**, No. 5, 485-493 (1999).
16. I. Nishizaki and S. Meiarashi, "Long-term deterioration of GFRP in water and moist environment," *J. Compos. Construct.*, **6**, No. 1, 21-27 (2002).
17. S. Kajorncheappunngam, R. K. Gupta, and H. V. S. GangaRao, "Effect of aging environment on degradation of glass-reinforced epoxy," *J. Compos. Construct.*, **6**, No. 1, 61-69 (2002).
18. A. Apicella, C. Migliaresi, L. Nicodemo, L. Nicolais, L. Iaccarino, and S. Roccotelli, "Water sorption and mechanical properties of a glass-reinforced polyester resin," *Composites*, 406-410 (October, 1982).
19. K. Van de Velde and P. Kiekens, "Effects of chemical environments on pultruded E-glass reinforced polyesters," *J. Compos. Technol. Res.*, **23**, No. 2, 92-101 (2001).
20. L. C. Bank, T. R. Gentry, and A. Barkatt, "Accelerated test methods to determine the long-term behavior of FRP composite structures: environmental effects," *J. Reinf. Plastics Compos.*, **14**, 559-587 (1995).
21. B. R. Bogner and P. P. Borja, "Ultra-violet light resistance of pultruded composites," in: *Proceedings of the European Pultrusion Technology Association (EPTA) Conference, Venice (1994)*.
22. I. Ghorbel and D. Valentin, "Hydrothermal effects on the physico-chemical properties of pure and glass fiber reinforced polyester and vinylester resins," *Polym. Compos.*, **14**, No. 4, 324-334 (1993).
23. R. Silverstein, C. G. Bassler, and T. C. Morrill, *Spectrometric Identification of Organic Compounds*, 3rd Ed., John Wiley & Sons (1974).
24. J. Lucki, J. F. Rabek, B. Ranby, and C. Ekstrom, "Photolysis of polyesters," *Eur. Polym. J.*, **17**, 919-933 (1981).

Copyright of *Mechanics of Composite Materials* is the property of Springer Science & Business Media B.V. and its content may not be copied or emailed to multiple sites or posted to a listserv without the copyright holder's express written permission. However, users may print, download, or email articles for individual use.